

EFFECT OF SLIP VELOCITY ON THE PERFORMANCE OF A SHORT BEARING LUBRICATED WITH A MAGNETIC FLUID

RACHANA U. PATEL, G. M. DEHERI*

Department of Mathematics, Sardar Patel University, Vallabh Vidyanagar – 388 120, Gujarat State, India.

* corresponding author: gm.deheri@rediffmail.com

ABSTRACT. This paper aims at analyzing the effect of velocity slip on the behavior of a magnetic fluid based infinitely short hydrodynamic slider bearing. Solving the Reynolds' equation, the expression for pressure distribution is obtained. In turn, this leads to the calculation of the load carrying capacity. Further, the friction is also computed. It is observed that the magnetization paves the way for an overall improved performance of the bearing system. However the magnetic fluid lubricant fails to alter the friction. It is established that the slip parameter needs to be kept at minimum to achieve better performance of the bearing system, although the effect of the slip parameter on the load carrying capacity is in most situations, negligible. It is found that for large values of the aspect ratio, the effect of slip is increasingly significant. Of course, the aspect ratio plays a crucial role in this improved performance. Lastly, it is established that the bearing can support a load even in the absence of flow, which does not happen in the case of a conventional lubricant.

KEYWORDS: short bearing, magnetic fluid, slip velocity, load carrying capacity.

1. INTRODUCTION

Pinkus and Sternlicht [1] presented an analysis for the hydrodynamic lubrication of slider bearings. Exact solutions of the Reynolds' equation for slider bearings with several film geometries have been treated in numerous books and research papers (Cameron [2], Archibald [3], Lord Rayleigh [4], Charnes and Saibel [5], Basu, Sengupta and Ahuja [6], Majumdar [7], Hamrock [8], Gross, Matsch, Castelli, Eshel, Vohr and Wildmann [9], Prakash and Vij [10]). Patel and Gupta [11] considered the effect of slip velocity on the hydrodynamic lubrication of a porous slider bearing. They showed that velocity slip decreased the load carrying capacity.

All these above studies considered conventional lubricants. Agrawal [12] dealt with the configuration of Prakash and Vij [10] with a magnetic fluid lubricant, and found that the performance was better than with a conventional lubricant. Bhat and Deheri [13] modified and extended the analysis of Agrawal [12] by considering a magnetic fluid based porous composite slider bearing with its slider consisting of an inclined pad and a flat pad. Bhat and Deheri established that the magnetic fluid increased the load carrying capacity, did not affect the friction, decreased the coefficient of friction, and shifted the centre of pressure towards the inlet. Patel et al. [14] analyzed the performance of a magnetic fluid based infinitely short bearing. It was shown that the magnetization sharply increased the load carrying capacity. The friction remained unchanged due to magnetization. Prajapati [15] investigated the performance of a magnetic fluid based porous inclined slider bearing with velocity slip, and concluded that the magnetic fluid lubricant minimized the negative effect of the velocity slip.

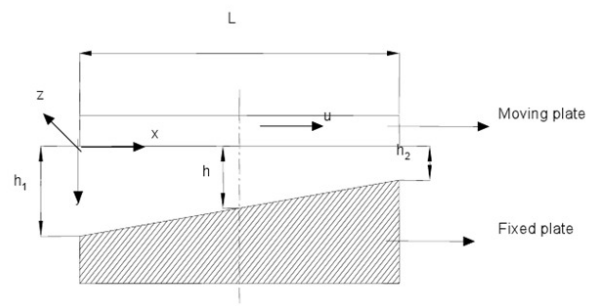


FIGURE 1. Configuration of the bearing system.

Recently, hydrodynamic lubrication of Short bearings have been subjected to investigations in Patel et al. [23], Vakis and Polycarpous [24] and Patel and Deheri [25].

The present study discusses the performance of a magnetic fluid based short bearing system with slip effect while the magnitude of the magnetic field is represented by a cosine function.

2. ANALYSIS

Figure 1 consists of the configuration of the bearing system, which is infinitely short in the Z -direction. The slider runs with uniform velocity u in the X -direction. The length of the bearing is L and the breadth B is in the Z -direction, where $B \ll L$. The pressure gradient $\frac{\partial p}{\partial x}$ can be neglected because the pressure gradient $\frac{\partial p}{\partial z}$ is much larger as a consequence of B being very small. The magnetic fluid is a suspension of solid magnetic particles approximately 3–10 nanometers in diameter stabilized by a surfactant in a liquid carrier. With the help of an external magnetic

field these fluids can be confined, positioned, shaped and controlled as desired. For details, see Bhat [22]. The magnetic field is taken to be oblique to the stator, as in Agrawal [12]. Following Bhat [22] and Prajapati [16], the magnetic field is taken as

$$\bar{H} = (H(z) \cos \phi, 0, H(z) \sin \phi); \quad \phi = \phi(x, z), \quad (1)$$

where the inclination angle of the magnetic field is described from the partial differential equation

$$\cot \phi \frac{\partial \phi}{\partial z} + \frac{\partial \phi}{\partial x} = 1 \frac{1}{H} \frac{dH}{dz}. \quad (2)$$

In view of the deliberation carried out in Prajapati [16], Verma [17] and Bhat and Deheri [18] the magnitude of the magnetic field is assumed to be of the form

$$H^2 = kB^2 \cos \frac{\pi z}{B},$$

where k is chosen to suit the dimensions of both sides and the strength of the magnetic field. Under the usual assumptions of hydrodynamic lubrication, and employing the Beavers and Joseph [19] model for slip, the governing Reynolds' equation (Agrawal [12], Prajapati [16], Patel et al.[14]) turns out to be

$$\frac{d^2}{dz^2} \left(p - \frac{\mu_0 \bar{\mu} H^2}{2} \right) = \frac{6\mu u(2 + sh)}{h^3(4 + sh)} \frac{dh}{dx}, \quad (3)$$

where μ_0 is the magnetic susceptibility, $\bar{\mu}$ is free space permeability, μ is lubricant viscosity and an m is the aspect ratio. The associated boundary conditions are

$$p = 0 \text{ at } z = \pm \frac{B}{2} \quad \text{and} \quad \frac{dp}{dz} = 0 \text{ at } z = 0. \quad (4)$$

The expression for pressure distribution is obtained by integrating Equation (3) with respect to the boundary condition (4), as

$$p = \frac{\mu_0 \bar{\mu} kB^2}{2} \cos \frac{\pi z}{B} - \frac{3\mu \mu m}{L h_2^2 t^3} \frac{2 + sh_2}{4 + sh_2} \frac{2 + 2sh_2 t + s^2 h_2^2 t^2}{(1 + sh_2 t)^2} \left(z^2 - \frac{B^2}{4} \right), \quad (5)$$

where $t = 1 + m(1 - x/L)$, while the aspect ratio m comes from $m = (h_1 - h_2)/h_2$.

Introduction of the dimensionless quantities

$$X = \frac{x}{L}, \quad P = \frac{h_2^3 p}{\mu u B^2}, \quad \mu^* = -\frac{h_2^3 k \mu_0 \bar{\mu}}{\mu u},$$

$$Y = \frac{y}{h}, \quad Z = \frac{z}{B}, \quad \bar{s} = sh_2$$

leads to the expression for the non-dimensional pressure distribution, obtained as

$$P = \frac{\mu^*}{2} \cos \pi Z - \frac{3mh_2}{L t^3} \frac{2 + \bar{s}t}{4 + \bar{s}t} \frac{2 + 2\bar{s}t\bar{s}^2 t^2}{(1 + \bar{s}t)^2} \left(Z^2 - \frac{1}{4} \right). \quad (6)$$

Then the load carrying capacity per unit width is determined from

$$w = \frac{\mu_0 \bar{\mu} kB^2 L}{\pi} + \frac{\mu u B^2}{2h_2^2} \left(\frac{19}{16} s^2 h_2^2 \ln(m+1) - \frac{3}{4} s h_2 \frac{m}{m+1} + \frac{1}{2} \frac{m(m+2)}{(m+1)^2} + \frac{5}{144} s^2 h_2^2 \ln \frac{4 + sh_2(m+1)}{4 + sh_2} - \frac{11}{9} s^2 h_2^2 \ln \frac{1 + sh_2(m+1)}{1 + sh_2} - \frac{1}{3} s^2 h_2^2 \left(\frac{1}{1 + sh_2} - \frac{1}{1 + sh_2(m+1)} \right) \right). \quad (7)$$

Thus, the dimensionless load carrying capacity of the bearing system comes out to be

$$W = \frac{h_2^3 w \pi}{\mu u B^4} = \pi \int_{-1/2}^{1/2} \int_0^1 P(X, Z) dX dZ = \frac{\mu^* L}{B \pi} + \frac{h_2}{2B} \left(\frac{19}{16} \bar{s}^2 \ln(m+1) - \frac{3}{4} \bar{s} \frac{m}{m+1} + \frac{1}{2} \frac{m(m+2)}{(m+1)^2} + \frac{5}{144} \bar{s}^2 \ln \frac{4 + \bar{s}(m+1)}{4 + \bar{s}} - \frac{11}{9} \bar{s}^2 \ln \frac{1 + \bar{s}(m+1)}{1 + \bar{s}} - \frac{1}{3} \bar{s}^2 \left(\frac{1}{1 + \bar{s}} - \frac{1}{1 + \bar{s}(m+1)} \right) \right). \quad (8)$$

The frictional force \bar{F} per unit width of the lower plane of the moving plate is obtained as

$$\bar{F} = \int_{-1/2}^{1/2} \bar{\tau} dZ, \quad (9)$$

where

$$\bar{\tau} = \frac{h_2}{\mu u} \tau \quad (10)$$

is the non-dimensional shearing stress, while

$$\tau = \frac{dp}{dz} \left(y - \frac{h}{2} \right) + \frac{\mu u}{h}. \quad (11)$$

A little computation indicates that

$$\bar{\tau} = \frac{\mu^* \pi \bar{B}}{2} \sin(\pi Z) T \frac{2 + \bar{s}T}{1 + \bar{s}T} \left(Y - \frac{1}{2} \right) - \frac{6mh_2 Z}{L} \frac{(2 + \bar{s}T)^2 (2 + 2\bar{s}T + \bar{s}^2 T^2)}{T(1 + \bar{s}T)^3 (4 + \bar{s}T)} \left(Y - \frac{1}{2} \right) + \frac{1 + \bar{s}T}{T(2 + \bar{s}T)}, \quad (12)$$

where $T = 1 + m(1 - X)$.

At $Y = 0$ (moving plate), one computes that

$$\bar{\tau} = \frac{\mu^* \pi \bar{B}}{4} \sin(\pi Z) T \frac{2 + \bar{s}T}{1 + \bar{s}T} \left(Y - \frac{1}{2} \right) - \frac{3mh_2 Z}{L} \frac{(2 + \bar{s}T)^2 (2 + 2\bar{s}T + \bar{s}^2 T^2)}{T(1 + \bar{s}T)^3 (4 + \bar{s}T)} \left(Y - \frac{1}{2} \right) + \frac{1 + \bar{s}T}{T(2 + \bar{s}T)}. \quad (13)$$

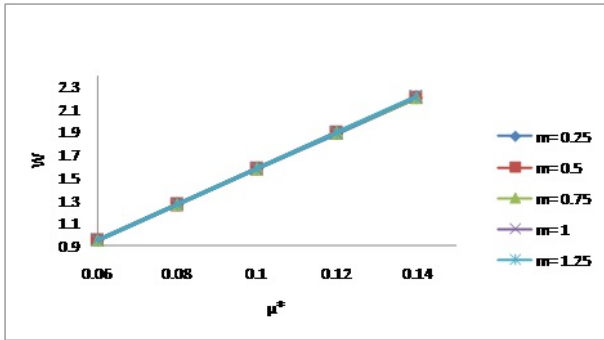


FIGURE 2. Variation of load carrying capacity with respect to μ^* and m .

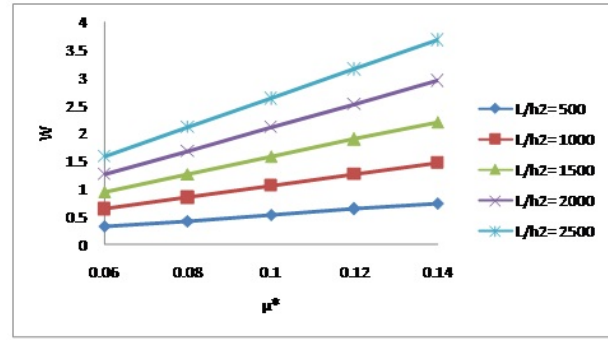


FIGURE 4. Variation of load carrying capacity with respect to μ^* and L/h_2 .

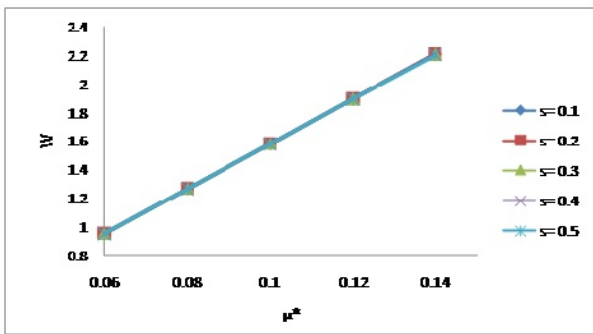


FIGURE 3. Variation of load carrying capacity with respect to μ^* and s .

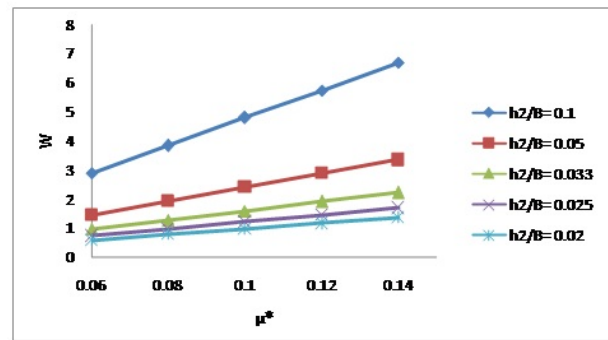


FIGURE 5. Variation of load carrying capacity with respect to μ^* and h_2/B .

Therefore, the friction force in non-dimensional form at the moving plate is calculated as

$$F_0 = \frac{1 + \bar{s}T}{T(2 + \bar{s}T)}. \tag{14}$$

Next, at $Y = 1$ (fixed plate), one concludes that

$$\begin{aligned} \bar{\tau} = & \frac{\mu^* \pi \bar{B}}{4} \sin(\pi Z) T \frac{2 + \bar{s}T}{1 + \bar{s}T} \left(Y - \frac{1}{2} \right) \\ & - \frac{3mh_2Z}{L} \frac{(2 + \bar{s}T)^2(2 + 2\bar{s}T + \bar{s}^2T^2)}{T(1 + \bar{s}T)^3(4 + \bar{s}T)} \left(Y - \frac{1}{2} \right) \\ & + \frac{1 + \bar{s}T}{T(2 + \bar{s}T)}, \end{aligned} \tag{15}$$

which transforms to the non dimensional form as

$$F_1 = \frac{1 + \bar{s}T}{T(2 + \bar{s}T)}. \tag{16}$$

It is clearly seen from Equations (14) and (16) that

$$F_0 = F_1. \tag{17}$$

3. RESULTS AND DISCUSSION

Equations (6) and (8), respectively, present the variation of non-dimensional pressure distribution and load carrying capacity, while the frictional force is determined from Equation (9). Comparison with the conventional lubricant indicates that the non-dimensional

pressure increases by

$$\frac{\mu^* \cos \pi Z}{2},$$

while the load carrying capacity enhances by

$$\frac{\mu^*(L/h_2)}{B/h_2}.$$

For lower values of the slip parameter, the load carrying capacity estimated here is approximately three times more than the load calculated from the investigation of Patel [20]. It is interesting to note that the friction remain unchanged in spite of the presence of slip, which is clear from Equation (17). However, for large values of the aspect ratio, the effect of slip on friction is significant.

The distribution of load carrying capacity with respect to magnetization μ^* for various values of m , s , L/h_2 and h_2/B is presented in Figures 2–5. All these figures make it clear that the load carrying capacity increases due to magnetization. Further, the load carrying capacity increases for increasing values of m , L/h_2 and h_2/B while it decreases with increasing slip velocity values. However, the effect of m and s on μ^* is negligible so far as the load carrying capacity is concerned. (Figures 2 and 3).

Figures 6–8 show the variation of load carrying capacity with respect to slip velocity s for different values of m , L/h_2 and h_2/B , respectively. It is clearly

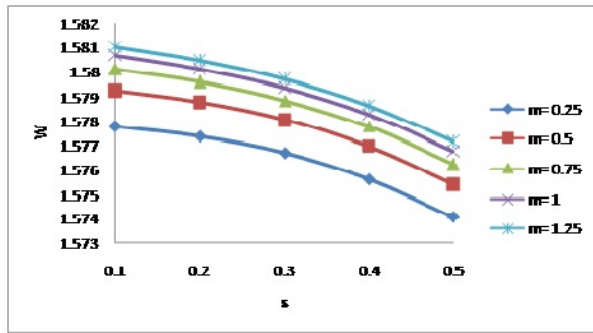


FIGURE 6. Variation of load carrying capacity with respect to s and m .

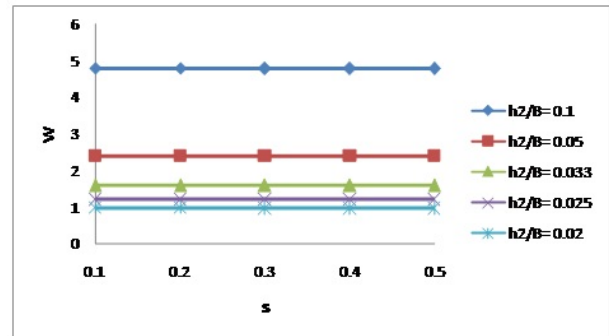


FIGURE 8. Variation of load carrying capacity with respect to s and h_2/B .

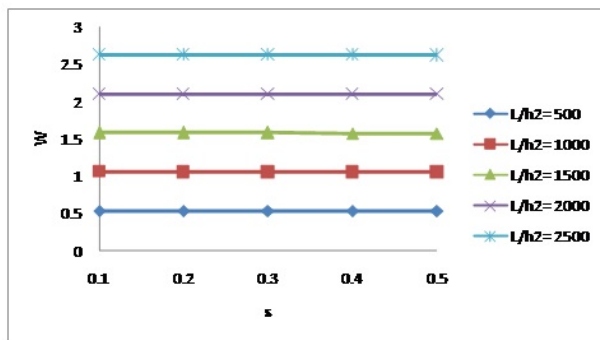


FIGURE 7. Variation of load carrying capacity with respect to s and L/h_2 .

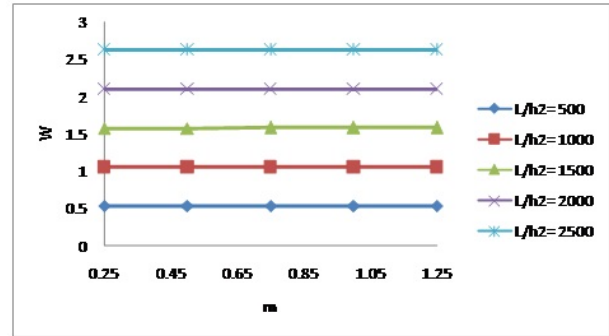


FIGURE 9. Variation of load carrying capacity with respect to m and L/h_2 .

seen from these figures that the load carrying capacity decreases with increasing slip velocity values. However, the decrease remains nominal, as can be seen from Figures 6–8.

Figures 9 and 10 deal with the distribution of load carrying capacity with respect to m . The load carrying capacity increases with increasing values of m . Figure 11 confirms that the rate of increase in load carrying capacity with respect to L/h_2 increases with increasing values of h_2/B . Thus, the combined effect of the two ratios L/h_2 and h_2/B is significantly positive. From Figure 12, it is found that the friction decreases with respect to the aspect ratio, whereas it increases with increasing slip parameter values.

4. CONCLUSIONS

This paper underlines that from the point of view life time of bearing, the slip parameter needs to be put at a minimum value. A comparison of our paper with the discussions of Patel et al. [21] indicates that the load carrying capacity remains almost identical for lower aspect ratio values. The industrial importance of this work is that it offers an additional degree of freedom from the design point of view, in terms of the form of the magnitude of the magnetic field. It is suggested that the adverse effect of slip velocity can be compensated to a large extent by the magnetic fluid lubricant, when a suitable aspect ratio value is chosen.

LIST OF SYMBOLS

- h Fluid film thickness at any point [mm]
- m Aspect ratio
- p Lubricant pressure [N/mm^2]
- u Uniform velocity in X-direction
- w Load carrying capacity [N]
- B Breadth of the bearing [mm]
- F Frictional force
- L Length of the bearing [mm]
- P Dimensionless pressure
- W Non-dimensional load carrying capacity
- h_1 Maximum film thickness [mm]
- h_2 Minimum film thickness [mm]
- \bar{F} Dimensionless frictional force
- F_0 Non-dimensional frictional force (moving plate)
- F_1 Non-dimensional frictional force (fixed plate)
- H Magnitude of the magnetic field
- \bar{H} Magnetic field
- ϕ Inclination angle of the magnetic field
- μ Lubricant viscosity [Ns/mm^2]
- τ Shear stress [N/mm^2]
- μ_0 Magnetic susceptibility
- $\bar{\mu}$ Free space permeability
- μ^* Dimensionless magnetization parameter
- $\bar{\tau}$ Dimensionless shear stress

REFERENCES

- [1] Pinkus, O., Sternlicht, B., Theory of Hydrodynamic Lubrication, McGrawHill, New York, 1961.

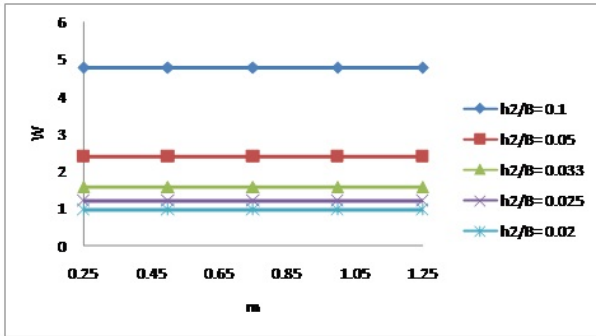


FIGURE 10. Variation of load carrying capacity with respect to m and h_2/B .

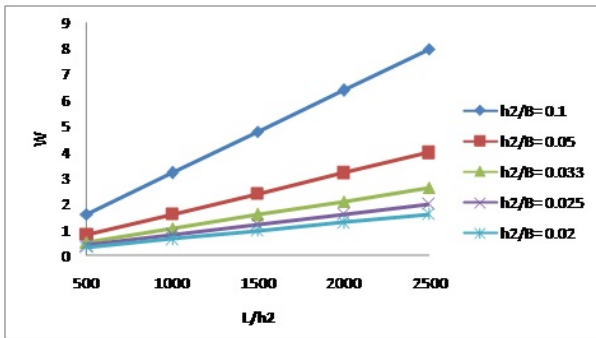


FIGURE 11. Variation of load carrying capacity with respect to L/h_2 and h_2/B .

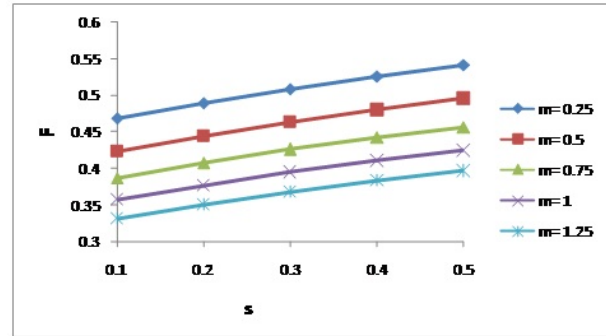


FIGURE 12. Variation of friction with respect to s and m .

[2] Cameron, A., The Principles of Lubrication, Longmans, London, 1996.

[3] Archibald, F. R., A Simple Hydrodynamic Thrust Bearing, ASME 72, 1950, p. 393.

[4] Lord Rayleigh, Notes on the Theory of Lubrication, Phil. Mag. 35, 1918, p. 1–12.

[5] Charnes, A., Saibel, E., On the Solution of the Reynolds' Equation for Slider Bearing Lubrication, Part 1, ASME 74, 1952, p. 867.

[6] Basu, S. K., Sengupta, S. N., Ahuja, B. B., Fundamentals of Tribology, Prentice-Hall of India Private Limited, New Delhi, 2005.

[7] Majumdar, B. C., Introduction to Tribology of Bearings, S. Chand and Company Limited, New Delhi, 2008.

[8] Hamrock, B. J., Fundamentals of Fluid Film Lubrication, McGraw-Hill, Inc. New York, 1994.

[9] Gross, W. A., Matsch Lee, A., Castelli, V., Eshel, A., Vohr, J. H., Wildmann, M., Fluid Film Lubrication, A Wiley-Interscience Publication, John Wiley and Sons, New York, 1980.

[10] Prakash, J., Vij, S. K., Hydrodynamic Lubrication of Porous Slider, Journal of Mechanical Engineering and Science 15, 1973, pp. 232–234.

[11] Patel, K. C., Gupta, J. L., Hydrodynamic Lubrication of a Porous Slider Bearing with Slip Velocity, WEAR 85, 1983, pp. 309–317.

[12] Agrawal, V. K., Magnetic Fluid-based Porous Inclined Slider Bearing, WEAR 107, 1986, pp. 133–139.

[13] Bhat, M. V., Deheri, G. M., Porous Composite Slider Bearing Lubricated with Magnetic Fluid, Japanese Journal of Applied Physics 30, 1991, pp.2513–2514.

[14] Patel, R. M., Deheri, G. M., Vadher, P. A., Performance of a Magnetic Fluid-based Short Bearing, Journal of Applied Sciences 7(3), 2010, pp. 63–78.

[15] Prajapati, B L., Magnetic Fluid-based Porous Inclined Slider Bearing with Velocity Slip, Prajna, 1994, pp.73–38.

[16] Prajapati, B L., On Certain Theoretical Studies in Hydrodynamics and Electro Magnetohydrodynamic Lubrication, Dissertation, S.P. University, Vallabh Vidhyanagar, 1995.

[17] Verma, P. D. S., Magnetic Fluid-based Squeeze Films, Int. J. Eng. Sci. 24(3), 1986, pp. 395–401.

[18] Bhat, M. V., Deheri, G. M., Squeeze Film Behavior in Porous Annular Discs Lubricated with Magnetic Fluid, WEAR 151, 1991, pp.123–128.

[19] Beavers, G.S. and Joseph, D.D., 1967, “Boundary conditions at a naturally permeable wall”, Jour. Fluid Mechanics 30, pp. 197–207.

[20] Patel, N.S., Analysis of Magnetic Fluid-based Hydrodynamic Slider Bearing, Thesis M. Tech., Sardar Vallabhbhai National Institute of Technology, Surat, 2007.

[21] Patel, N. D., Deheri, G. M., Effect of surface roughness on the performance of a magnetic fluid based parallel plate porous slider bearing with slip velocity, Journal of the Serbian for computational Mechanics 5, 2011, pp. 104–118.

[22] Bhat, M.V., Lubrication with magnetic fluid, Team Sprit, India, Pvt. Ltd., 2003.

[23] Patel, N.S., Vakharia, D.P., Deheri, G. M., A Study on the Performance of a Magnetic-Fluid-Based Hydrodynamic Short Journal Bearing, ISRN Mechanical Engineering, 2012, Article ID 603460.

[24] Vakis, A.I., Polycarpou, A.A., An Advanced Rough Surface Continuum-Based Contact and Sliding Model in the Presence of Molecularly Thin Lubricant, Tribology Letters, 49(1), 2013, pp. 227–238.

[25] Patel, J.R., Deheri, G.M., A Comparison of Porous Structures on the Performance of a Magnetic Fluid Based Rough Short Bearing, Tribology in Industry, 35(3), 2013, pp. 177–189.